The Catalytic Use of Onion-Like Carbon Materials for the Styrene Synthesis by Oxidative Dehydrogenation of Ethylbenzene.

Nicolas Keller, Nadezhda I. Maksimova, Vladimir V. Roddatis, Michael Schur, Gerhard Mestl, Yurii V. Butenko, Vladimir L. Kuznetsov and Robert Schlögl[?]

Since the discovery of fullerenes in 1985,[1] the chemistry of sp^2-hybridised nanostructured carbon has received an increasing interest both from a fundamental point of view and for potential applications. It has stimulated the synthesis of a large variety of new fullerene-related materials (giant fullerenes, nanotubes, nanospheres, nanocones, nanofolders, nanobundles, onion-like carbon, etc).[2] Unique chemical and physical properties suggest

---

Dr. Nicolas Keller, Nadezhda I. Maximova, Dr. Vladimir V. Roddatis, Dr. Michael Schur, Dr. Gerhard Mestl,[?] Prof. Dr. R. Schlögl, Abteilung Anorganische Chemie, Fritz-Haber-Institut der Max-Planck-Gesellschaft, Faradayweg 4-6, D-14195 Berlin, Germany, Telefax: +49 (0)30 8413 4401, e-mail: Schloegl@fhi-berlin.mpg.de.

Dr. Yurii V. Butenko, Dr. Vladimir L. Kuznetsov, Boreskov Institute of Catalysis, Lavrentieva 5, 630090 Novosibirsk, Russian Federation.

novel applications, including nanoscale engineering and electronics, optoelectronic sensors, three-dimensional composite materials, microfilters, magnetic materials and catalysis.[3] Research on onion-like carbons (OLC) is confined to the development of synthesis methods and to the description of physical and chemical properties.[4] These closed spherical carbon shells, however, could also provide interesting catalytic properties due to the almost perfect graphitic network with a high degree of curvature.

Direct dehydrogenation of hydrocarbons is used in numerous industrial processes. Due to their endothermic character, such processes are limited by thermodynamic limitations calling for alternatives. In case of styrene synthesis, one of the ten most important industrial processes, the exothermic oxidative dehydrogenation of ethylbenzene (ODH) is an elegant and promising reaction, for which carbon catalysts already proved their efficiency.[5,6] The porosity of carbon catalysts used so far seems to play a negative role by hindering the styrene desorption. This limits the ethylbenzene conversion and leads to non-selective, consecutive reactions.[5,7] Therefore, OLC are valuable candidates, due to the absence of inner particle porosity, as compared to other forms of carbon materials.[8]

Figure 1 displays the catalytic behaviour of the OLC material on a mass referenced basis for the ODH of ethylbenzene to styrene with time on stream. For comparison, the steady state yields on a catalyst mass basis are also shown, which were obtained over the industrial K-Fe catalyst and other forms of carbon. The OLC catalyst exhibited a minor initial activity developing into conversion levels of 92 % after an activation period of about 2 hours on stream. The stable styrene selectivity of 68 % allowed high styrene yields of 62 %. The performance of OLC in ODH is not limited by conversion as in case of traditional K-promoted iron oxide systems, for which thermodynamic constraints of dehydrogenation limit an increase of the styrene yield above 50 %.[9,10]

Figure 2A displays high resolution transmission electron micrographs of fresh OLC. Image a of Fig. 2A shows clean, multi-shell particles with an interlayer distance close to 0.35 nm, typical for sp^2 hybridised carbon structures. The inset of Fig. 2a shows one example for a well resolved OLC. The contrast variations of this OLC indicate intact graphene layers and structurally less-defined areas at the curvature of OLC (indicated by arrows). Image b of Figure 2A displays OLC material after catalysis for 40 h. The OLC

seem to be disintegrated into more or less disorganized carbon. The difference in contrast as compared to the image prior to catalysis confirmed that the carbon onions did not have well defined structures anymore.

X-ray diffraction was further used to characterize the structure of OLC before and after catalysis. Fig. 2B shows the XRD data obtained for fresh (pattern a, dotted line) and used (pattern b, full line) OLC. The diffractogram of fresh OLC (Fig. 2B, a) is characteristic for graphite-like material with a high degree of stacking faults as expected. For comparison, the theoretical pattern of hexagonal graphite is indicated by the vertical lines with the respective indexing. The diffractogram recorded after catalysis (Fig. 2B, b) proves the generation of diamond-like-carbon (DLC) material, i.e. sp^3 carbon, during the styrene reaction. The peaks at 43.9 and 75.3 2T coincide with the 111 and 220 reflections of diamond as indicated by the vertical lines. Hence, it can be concluded that part of the ill-defined material detected by HR-TEM and Raman spectroscopy is DLC.

Raman spectroscopy further revealed the nature of this ill-defined carbon. Figure 2C shows the raw spectra obtained from the fresh (spectrum a) and used (spectrum b) OLC on its left side. The deconvolution of these spectra is

displayed on the right side. The Raman spectrum of fresh OLC (Fig. 2C, spectrum a) exhibits the Raman bands characteristic for disordered (D: 1318 cm^{-1}, and D': 1594 cm^{-1}) and ordered (G: 1573 cm^{-1}) graphene structures[11]. This Raman spectrum is in agreement with the HR-TEM analysis which revealed intact graphene layers and ill-defined structures at the curvatures of OLC (Fig. 2A, image a) and the XRD data (Fig. 2B, pattern a). The intense Raman signature of the D (1328 cm^{-1}) and D' (1594 cm^{-1}) bands of the catalyst subsequent to reaction, completely overwhelming the G band at 1573 cm^{-1}, clearly evidenced a pronounced presence of disordered carbon structures after the catalytic test. The intensity increase of the two D and D' Raman signals was accompanied by a broadening and a slight blue-shift of the D band. The deconvolution additionally revealed a very broad background contribution to this band due to C-H, C-C deformations.[12] This very broad D band does not exclude the presence of sp^3-hybridised carbons after reaction as indicated by XRD (Fig 2B, pattern b).[12] Indeed, IR spectroscopy (spectra not shown) revealed the presence of C-H valence bands at 2920 cm^{-1} after catalysis together with bands at 1740, 1175 and 1090 cm^{-1} indicating the presence of basic C=O and C-O groups, respectively.

In addition to Raman spectroscopy and XRD, temperature-programmed combustion confirmed the presence of these two carbon species (Figure 3). As compared to the fresh, well-organized sp^2 hybridised OLC (a), the used active catalyst displayed a composite signal (b), which evidenced disordered sp^2/sp^3 carbon with a maximum combustion rate at around 850 K, in agreement with the reference, amorphous activated charcoal. The contribution to combustion at higher temperatures was assigned to remaining ordered sp^2 carbon structures. The water release simultaneous to the low temperature combustion peak confirmed the presence of hydrogen atoms in the highly disordered carbon, as indicated by IR spectroscopy.

Fig. 4 shows the O1s and C1s XP spectra obtained for the fresh and used OLC material. X-ray photoemission spectroscopy proved that the almost oxygen-free carbon surface of the fresh OLC (spectrum a of Fig. 4A) was transformed after reaction into an oxygen containing surface (open circles, Fig. 4A). The O 1s spectrum after reaction can be deconvoluted into two signals. The first is due to chinoidic carbonyl functions with a binding energy (B.E.) of 530.9 eV,[13] similar to spectra reported for other active carbon catalysts.[6,8] The dehydrogenating power of the catalyst thus seems to be linked to the

generation of these strongly basic sites during activation. The second with a B.E. of 533.4 eV arises from water adsorbed during transport through air. The C1s spectra (Fig. 4B) indicated the presence of oxidized carbon by an increased intensity at the high energy wing of the C1s signal. The inset of Fig. 4B shows the difference spectrum of used OLC (full line) and fresh OLC (dotted line). Its deconvolution confirmed presence two contributions at 288.2, indicative for basic, chinoidic surface groups, and 286.0 eV due to C-O groups. This XPS finding is in agreement with the IR observations mentioned above. Additionally, the graphitic C1s line at 284.4 eV was considerably broadened after catalysis proving the presence of structurally ill-defined carbon in line with Raman, XRD and TG-TPO.

The structural characterisation reveals that the function of the OLC carbon as ODH catalyst is uniquely related to its microstructure. The starting material, intact OLC with a large surface abundance of graphitic (0001) facets combined with a small abundance of edge/kink sites where the bending of the graphene layers occurs (blurred contrast in the TEM), is characterized by the complete absence of surface oxygen functionalities. In addition, the catalytic

test revealed that this material does not show initial catalytic activity. Catalytic activity develops with time on stream. XPS characterization proves the generation of strongly basic, chinoidic surface functionalities on the active carbon catalyst. It is suggested that these basic dehydrogenating surface groups are generated as the resonance stabilised C=O surface terminations of the edge/kink regions of OLC as described earlier.[7] This oxidation of the edge/kink sites is also seen as being responsible for the disintegration of the OLC during catalysis. The catalytic activity develops with increasing formation of these basic functionalities and accordingly increasing OLC disintegration. Hence, it may be questioned whether OLC are catalytically active at all. Comparative experiments with ultradispersed diamond (UDD), however, revealed that the DLC material detected by XRD after catalysis cannot account for the catalytic activity of OLC (data not shown). UDD are initially also completely inactive, like OLC, but their selectivity, which developed with time, is different from that of OLC, giving benzene as the main product.

The fact that carbon derived from OLC is superior in its performance on a mass referenced basis compared to other forms of carbon[8] (Styrene yields in % in Figure 1:

graphite 45, carbon filaments 53, OLC 62) evidences that this type of carbon contains a higher number of active sites per unit weight at steady state. This superior performance is also related to the optimised distribution of the sites required for oxygen activation (basal planes) and Broensted basic centres[9] (prismatic planes) on this type of nanocarbon.

The presence of disordered, sp^2 and sp^3 polymeric carbon resulting from unwanted styrene polymerisation is characteristic of all catalytic systems tested so far.[9,14] Its voluminuous and defective character makes it, however, particularly susceptible to oxidation in situ as evidenced by the data in Figure 3. A large difference in specific reactivity of the soft coke[15] to the carbon catalyst is a prerequisite for stable operation as the formation of coke cannot be completely avoided. By reducing the basic sites required for polymerisation to the minimum necessary for activating the EB substrate, the tendency for coke formation is smaller on carbon than on (potassium promoted) metal oxide systems.

The present data reveal that a significant potential for catalytic application lies in unpromoted nanocarbon materials if their microstructure can be tailored to support the optimum distribution of electron donating and

proton activating functions. The chemical simplicity of carbon and the unique property that deactivated surfaces gasify themselves in ODH reactions not only renders them well-suited model systems but also allow for realistic expectations of a technical application in heterogeneous catalysis. The synthetic limitations of the present OLC model system may be overcome by tailoring other more abundant forms of carbon into the desired target structure by synthetic[16] and post-synthetic thermochemical procedures.

Experimental Section

Concentric graphitic shell structures, known as Onion-Like Carbons (OLC), were produced by thermal annealing of Ultra-Dispersed Diamond (UDD) powder at 2140 K and at a 10^{-6} torr vacuum, according to the method developed by Kuznetsov at al.[17]

The reaction was carried out in a tubular quartz reactor of 4 mm inner diameter and 200 mm length. The catalyst (0.04 g) was placed in the isothermal oven zone between quartz wool plugs. He and O_2 were fed by mass flow controllers. Ethylbenzene (EB) in flowing He was provided by a saturator

kept at the required temperature (35°C, corresponding to 2,16 kPa) and mixed to the O_2-flow to obtain the EB to O_2 ratio of 1:1. The reaction was conducted at 790 K with an inlet EB concentration of 2 vol.% and a Liquid Hourly Space Velocity (LHSV) of 0.5 h^{-1}. The inlet and outlet gas analysis was carried out on-line by a gas chromatograph using a packed column (5% SP-1200/1.75% Bentone 34) for hydrocarbons and a capillary column (Carboxen 1010 PLOT) for permanent gases, respectively, coupled to FID and TCD detectors.

Transmission electron micrographs were taken on a Phillips CM200-FEG at an acceleration voltage of 200kV. Photoelectron spectra were recorded with a modified Leybold Heraeus spectrometer (LHS12 MCD) with Mg $K_?$ radiation (1253.6 eV) at a power of 240 W. The bandpass energy was set to 50 eV. X-ray satellites and Shirley background were subtracted. Thermal gravimetry analysis was performed on a Netzsch STA 449C balance, with a heating rate of 10 $K.min^{-1}$ and using a 20 % (v/v) O_2/He mixture, and coupled to a QMS200 mass spectrometer (Thermostar, Pfeiffer Vacuum). Raman spectra were recorded with a LabRam spectrometer (Dilor). The spectral slit width was set at 500 ?m giving a spectral resolution of 5 cm^{-1}. A He/Ne laser at 632.8 nm was used as the excitation source. IR spectra in diffuse

reflectance were recorded on a Bruker IFS-66 FT-IR spectrometer. XRD was performed on a Stoe Theta-Theta diffractometer in reflection. Cu K_a radiation was used.

References

[1] H.W. Kroto, J.R. Heath, S.C. O'Brien, R.F. Curl, R.E. Smalley, *Nature* **1985**, *318*, 162.

[2] a) S. Iijima, *Nature* **1991**, *354*, 56; b) D. Ugarte, *Nature* **1992**, *359*, 670; c) H. O'Pierson, *Handbook of Carbon, Graphite, Diamond and Fullerenes. Properties, Processing and Applications*, Noyes Publications, Park Ridge, **1993**; d) M. Jose-Yacamau, H. Terrones, L. Rendou, J.M. Dominguez, *Carbon* **1995**, *33*, 669; e) *Carbon nanotubes: preparation and properties* (Ed.: T.W. Ebbesen), CRC, Boca Raton, **1997**; f) M. Knupfer, *Surface Science Reports* **2001**, *42*, 1, and references therein.

[3] a) M. Terrones, W. Kuang Hsu, H.W. Kroto, D.R.M. Walton, *Topics in Current Chemistry* **1999**, *199*, 189, and references therein; b) P.M. Ajayan, O.Z. Zhou in *Carbon Nanotubes. Synthesis, Structure, Properties and Applcations*, Topics in Applied Physics, Vol. 80 (Eds.: M.S. Dresselhaus, G. Dresselhaus, Ph. Avouris), Springer, Heidelberg, **2001**, pp.391-425.

[4] a) D. Ugarte, *Carbon* **1995**, *33(7)*, 989; b) V.L. Kuznetsov, Yu.V. Butenko, A.L. Chuvilin, A.I. Romanenko, A.V. Okotrub, *Chem. Phys. Lett.* **2001**, *336*, 397.

[5] M.F.R. Pereira, J.J.M Orfao, J.L. Figueiredo, *Appl. Catal. A: General* **1999**, *184*, 153.

[6] G. Mestl, N.I. Maksimova, N. Keller, V.V. Roddatis, R. Schlögl, *Angew. Chem.* **2001**, *113(11)*, 2122; *Angew. Chem. Int. Ed.* **2001**, *40(11)*, 2066.

[7] a) C. Kuhrs, Y. Arita, W. Weiss, W. Ranke, R. Schlögl, *Topics in Catalysis* **2001**, *14(1-4)*, 111; b) J.A. Maciá, D. Cazorla Amorós y A. Linares Solano, *Proceedings of the Reunión de la Sociedad Espanola de Catálisis SECAT'01*, **2001**, pp.97-98.

[8] a) A more detailed comparison of the performances obtained with different forms of carbon will be given in a coming extended paper; b) Storage in air and transfer to the XPS chamber led to a second contribution due to adsorbed water.

[9] G. Emig, H. Hofmann, *J. Catal.* **1983**, *84*, 15.

[10] F. Cavani, F. Trifiro, *Appl. Catal. A: General* **1995**, *133*, 219.

[11] a) R.P. Vidano, D.B. Fishbach, L.J. Willis, T.M. Loehr, *Solid State Commun.* **1981**, *39*, 423; b) M.S.

Dresselhaus, G. Dresselhaus, *Adv. Phys.* **1981**, *30*, 139; c) Y. Kawashima, G. Katagiri, *Phys. Rev. B* **1995**, *52*, 10053.

[12] D. Espinat, H. Dexpert, E. Freund, G. Martino, M. Couzi, P. Lespade, F. Cruege, *Appl. Catal.* **1985**, *16*, 343.

[13] a) H. Ago, T. Kugler, F. Cacialli, W.R. Salaneck, M.S.P. Shaffer, A.H. Windle, R.H. Friend, *J. Phys. Chem. B* **1999**, *103*, 8116; b) M. Voll, H.P. Boehm, *Carbon* **1971**, *9*, 481.

[14] G.E. Vrieland, *J. Catal.* **1988**, *111*, 14.

[15] R. Schlögl in *Handbook of Heterogeneous Catalysis*, *Vol. 1* (Eds.: G. Ertl, H. Knözinger, J. Weitkamp), Wiley-VCH, Weinheim, **1997**, pp.138-191.

[16] C. Pham-Huu, N. Keller, V.V. Roddatis, G. Mestl, R. Schlögl, M.J. Ledoux, submitted to *Phys. Chem.-Chem. Phys.*

[17] a) V.L. Kuznetsov, A.L. Chuvilin, Yu.V. Butenko, I.Y. Mal'kov, V.M. Titov, *Chem. Phys. Lett.* **1994**, *222*, 343; b) V.L. Kuznetsov, A.L. Chuvilin, E.M. Moroz, V.N. Kolomiichuk, Sh.K. Shaikhutdinov, Yu.V. Butenko, *Carbon* **1994**, *32(5)*, 873.

Figure Captions

Fig. 1.

Performance of OLC in the ODH of ethylbenzene at 790 K with time on stream. X in % = ethylbenzene conversion (✍), selectivity to styrene (✍) and styrene yield (¦). Steady state styrene yields for graphite (Gr.), carbon nanofilaments (CNF) and the technical K-Fe catalyst are also given.

Fig. 2

A High resolution TEM images of OLC (a) prior and (b) subsequent to oxidative dehydrogenation of ethylbenzene. The inset of Fig. 2a shows the magnification of a single, intact OLC. The arrows indicate the blurred regions with less ordered structure

B X-Ray diffractograms of the OLC material prior (a) and subsequent (b) to catalysis. The theoretical positions and indices of reflections of graphite (G) and Diamond (D) are shown for comparison.

C Left side: original Raman spectra of OLC prior (a) and subsequent (b) to ODH of ethyl benzene. Right side:

deconvolutions of the Raman spectra prior (a) and subsequent (b) to catalysis.

Fig. 3

Differential Thermal Gravimetry of the temperature-programmed combustion of OLC (a) prior, (b) subsequent to ODH of ethyl benzene (T=temperature), (c) amorphous carbon (Norit A, Aldrich), and (d) graphite (SFG6, Timcal AG). (Below) Mass spectrometer trace of water formed during the combustion of OLC subsequent to catalysis.

Fig. 4

A O1s XP spectra of the OLC prior (solid line) and subsequent (open circles) to catalysis. The deconvolution into two contributions with B.E. of 531.1 and 533.4 eV is shown too.

B C1s XP spectra of OLC prior (dashed line) and subsequent (full line) to catalysis. The inset shows the deconvolution of the difference C1s spectrum into three contributions with BE of 288.2, 286.0 and 284.4 eV.

Short text for content:

The first use of onion-like carbons in the field of catalysis opens new routes for potential applications of non-planar carbon materials. An example is given with the oxidative dehydrogenation of ethylbenzene.

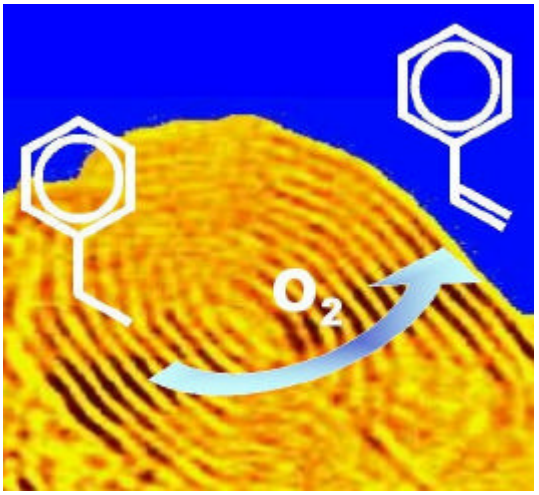

Keywords:

Ethylbenzene dehydrogenation, onion-like carbon, catalysis, oxygen functionalities.

Figure 1

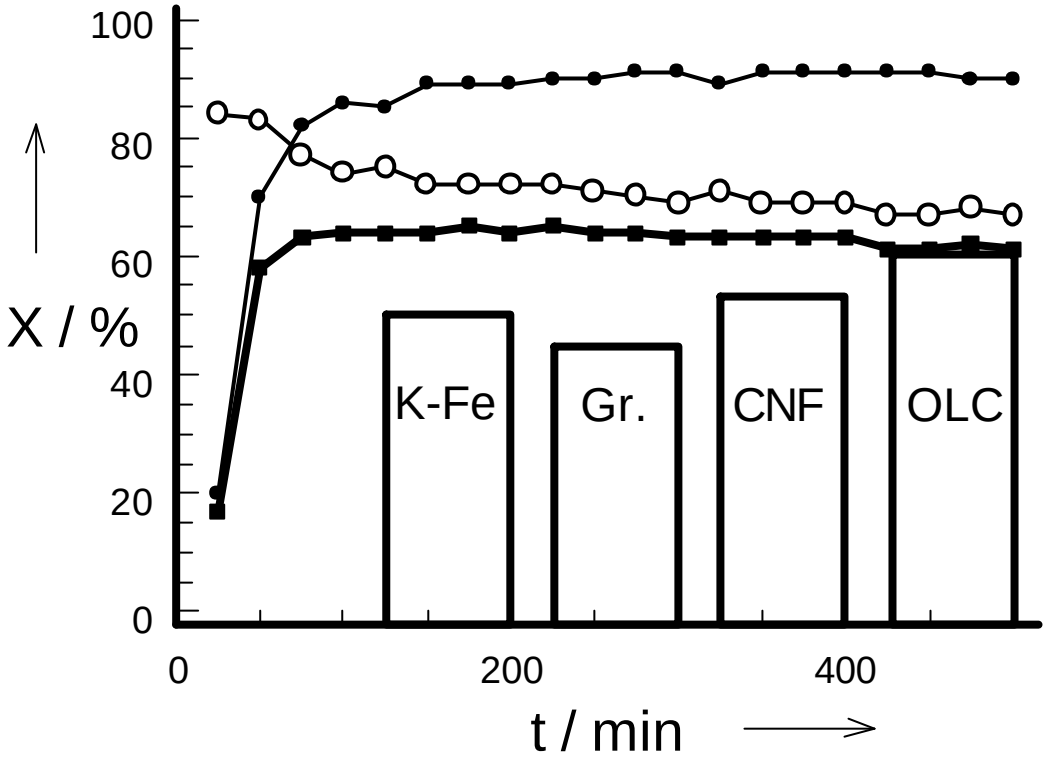

Figure 2

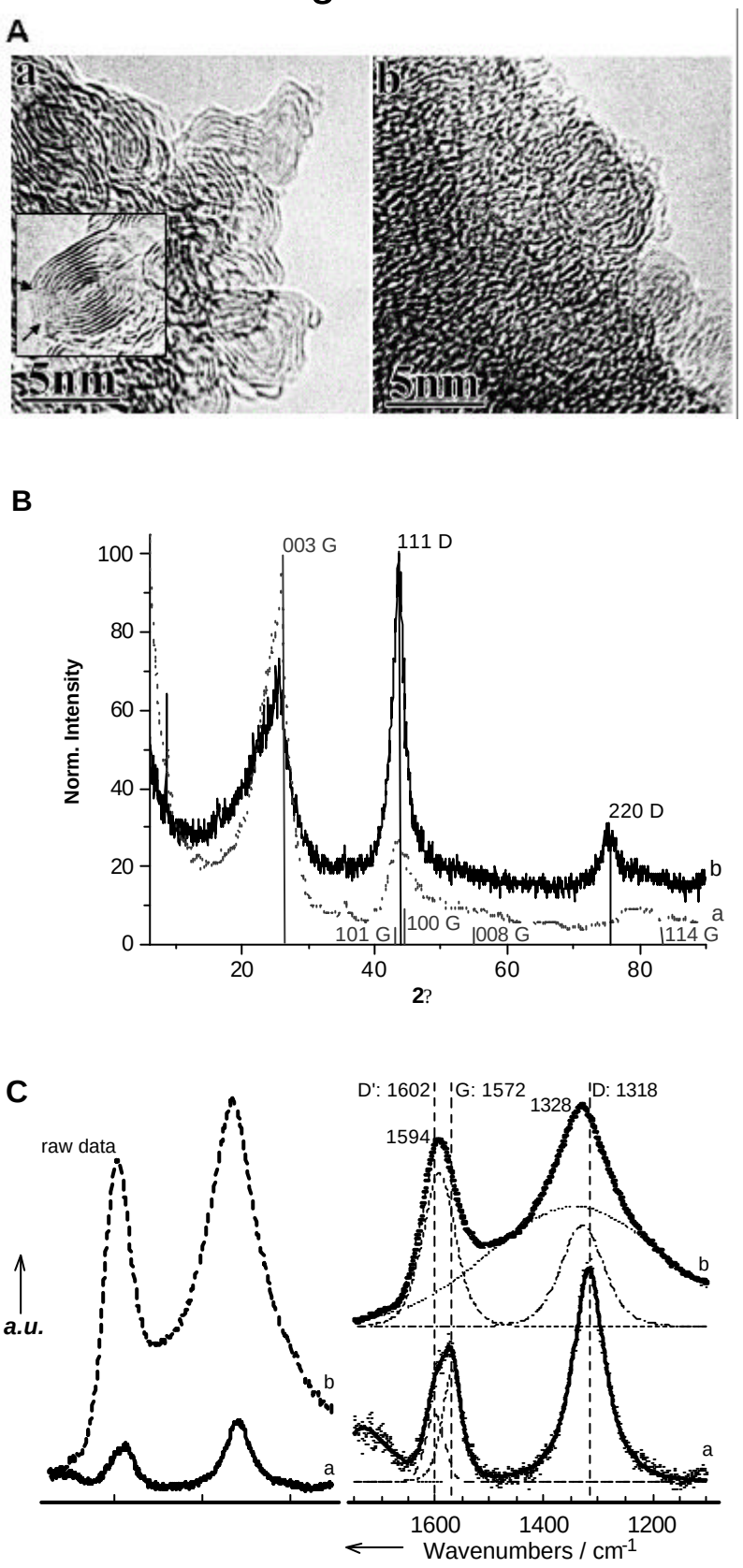
A
a
b
5nm
5nm
B
003 G
111 D
220 D
101 G
100 G
008 G
114 G
Norm. Intensity
2?
C
raw data
a.u.
D': 1602
G: 1572
D: 1318
1328
1594
Wavenumbers / cm-1

Figure 3

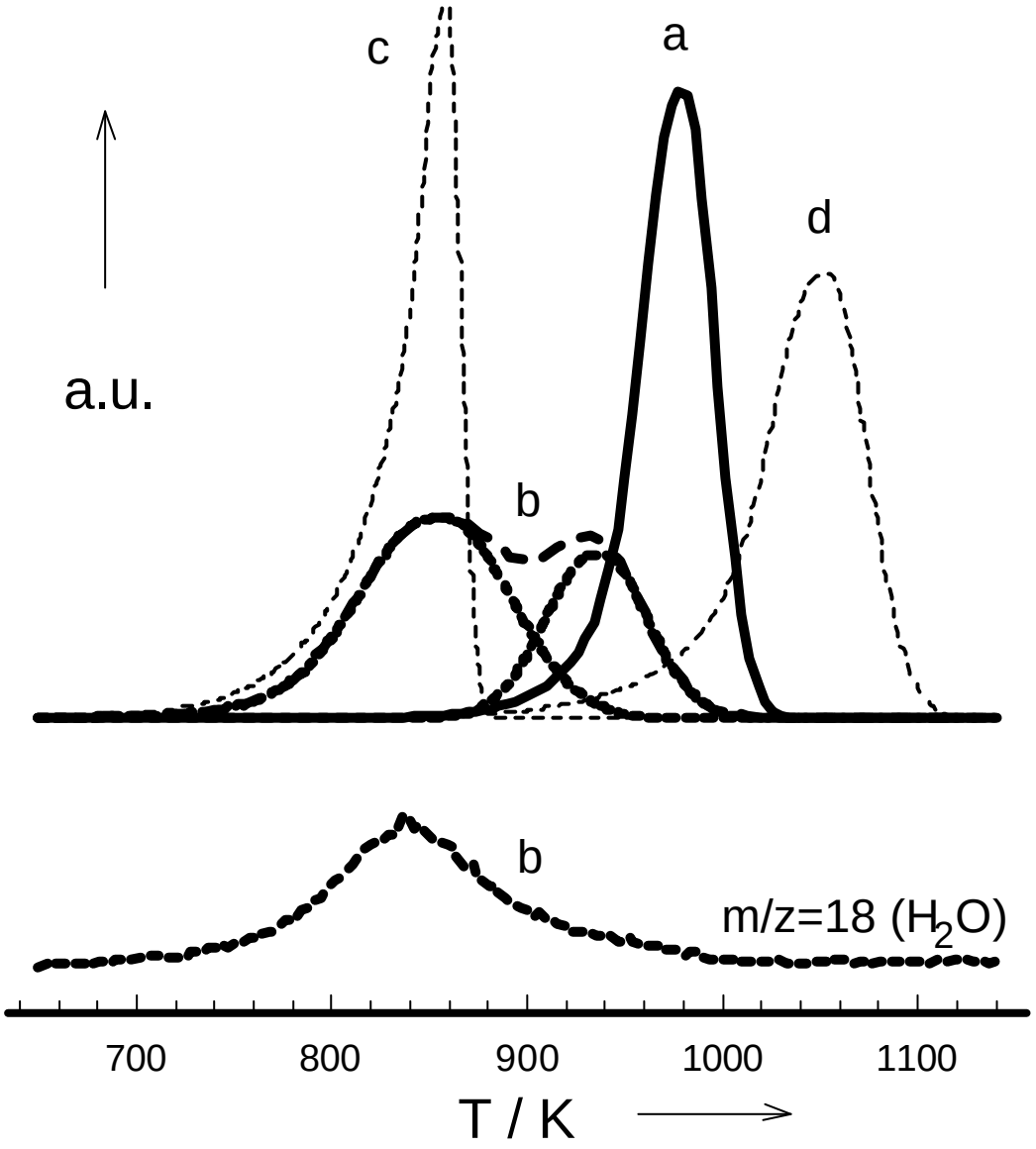

Figure 4